



## ***In silico* Exploration of Quinazolinone-incorporated-chalcones as EGFR inhibitors (T790M mutated) to Combat Lung Cancer**

**PRAVEEN KUMAR ARORA<sup>1\*</sup>, SUSHIL KUMAR<sup>2</sup>, SANDEEP KUMAR BANSAL<sup>3</sup>  
and TARUN VIRMANI<sup>4</sup>**

<sup>1</sup>Pt. L.R. College of Pharmacy, Faridabad, 121004, Haryana, India.

<sup>2</sup>School of Pharmaceutical Sciences, IFTM University, Moradabad-244001, Uttar Pradesh, India.

<sup>3</sup>Ram-Eesh Institute of Vocational and Technical Education, Greater Noida-201310, Uttar Pradesh, India.

<sup>4</sup>Department of Pharmaceutical Sciences, AMITY University, Greater Noida-201308, Uttar Pradesh, India.

\*Corresponding author E-mail: procarora@gmail.com

<http://dx.doi.org/10.13005/ojc/400521>

(Received: August 16, 2024; Accepted: October 14, 2024)

### **ABSTRACT**

The current research concentrates on the *in silico* exploration of quinazolinone-incorporated chalcones (42 ligands) as anti-lung-cancer agents by evaluating their ability to inhibit mutated EGFR (T790M mutation) by docking studies employing autodock 4. The observed free binding energies of the ligands were -45.44 KJ/mol to -34.64 KJ/mol and the observed inhibition constants range was 11.04 nM to 853.47 nM. In the docking studies, when compared with the reference EGFR TKIs (erlotinib, afatinib, and naquotinib), all the docked 42 ligands were found to have higher potency and the compound C19 was found as the most potent ligand (binding energy = -45.44 KJ/mol and inhibition constant = 11.04 nM). As per the Osiris property explorer prediction, ligand C6 was with the highest drug score (0.42) followed by ligand C9(0.35).

**Keywords:** Docking, EGFR inhibitors, Anticancer agents, Non-small cell lung cancer (NSCLC), Cytotoxicity, Chalcones, Quinazolinone.

### **INTRODUCTION**

Globally, lung cancer is the most prevalent cancer to be diagnosed and the primary cause of cancer-related mortality<sup>1,2</sup>. The substantial therapeutic potential of the quinazolinone/quinazoline scaffold was discovered through a review of the literature. Recently, certain new trimethoxy quinazolines have been identified by Altamimi *et al.*, as promiscuous EGFR inhibitors<sup>3</sup>.

Chalcones serve as an important

pharmacophoric site in a variety of anticancer compounds, such as butein, isoliquiritigenin, and other natural and synthetic anticancer compounds<sup>4</sup>. The chalcone structural motif (1,3-diaryl-prop-2-ene-1-one) exhibits a variety of biological activities. Molecular hybridization, a method of drug designing, involves joining two distinct bioactive scaffolds to create a single hybrid molecule. The design of new anticancer drugs have been shown to benefit greatly from the molecular hybridization approach, for example, para-aminoquinazoline-chalcone conjugates<sup>5</sup>, quinoline incorporated chalcones<sup>6</sup>,



benzimidazole incorporated chalcones<sup>7</sup>, chalcones having thiazole heterocyclic ring<sup>8</sup>, chalcones having thiazole ring<sup>9</sup>, 2-arylquinazolin-4-one naphthylchalcone hybrids<sup>10</sup>, 2-(4-methoxyphenyl) quinazolin-4-one-chalcone derivatives<sup>11</sup> etc., All favour employing the chalcone structural motif in the search for novel anticancer medicines.

Patients with lung cancer typically have a poor prognosis and a low survival rate, and this is largely due to EGFR over-expression and EGFR mutation. The harsh side effects and poor prognosis connected with traditional chemotherapeutic therapies have been the impetus for the creation of EGFR-TKIs<sup>12-14</sup>. First, second, and third-generation EGFR inhibitors are presently employed for treating NSCLC<sup>15</sup>. When treating NSCLC associated with the T790M EGFR mutation, first-generation (e.g. erlotinib) and second-generation (e.g. afatinib) EGFR inhibitors produce unsatisfactory results<sup>15</sup>. In clinical studies, it has been revealed that T790M mutation is also induced by first or second-generation EGFR TKIs<sup>15</sup>. At present, EGFR with T790M mutation can only be targeted satisfactorily by the third-generation EGFR TKIs (e.g. naquotinib, osimertinib or lazertinib) but in the course of treatment, these drugs also suffered from EGFR resistance<sup>15</sup>. The present study concentrates on the insilico investigations of the chalcone ligands to assess their toxicity risks, drug score, drug-likeness, physiochemical parameters, pharmacokinetic parameters, and their ability to inhibit mutated EGFR, taking erlotinib, afatinib and naquotinib as reference drugs for the comparison.

## MATERIALS AND METHODS

Osiris property explorer was used to predict toxicity risks, solubility, cLogP, TPSA, drug-likeness and drug-score. The Swiss ADME online server was used to predict the pharmacokinetic parameters. MarvinSketch18.23 was utilized for drawing chemical structures of ligands and for optimization of their energy. The T790M mutation carrying epidermal growth factor receptor (EGFR) (Protein data bank ID: 5Y9T) was obtained from the Protein data bank (<https://www.rcsb.org>). AutoDock 4.0 MGL tools were used to investigate molecular docking. Using the discovery studio visualizer, the ligand-EGFR (5Y9T) complex was observed.

### Docking run (TARGET 5Y9T)

Preparation of target protein (5Y9T) and the preparation of ligands were done as per the reported procedures<sup>10</sup>. Validated docking experiments using autodock 4 were done as per the reported procedure<sup>11</sup>.

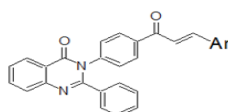
## RESULTS AND DISCUSSION

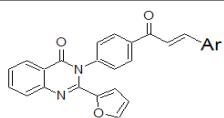
### Osiris property explorer toxicity predictions

The OSIRIS property explorer predicts the results using color code. The red and orange colors indicate that ligand is associated with high risk and medium risk of undesired effects (mutagenicity, tumorigenicity, irritant, and reproductive effect) respectively. Whereas a green color rules out such undesired effects (Table 1).

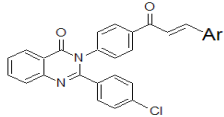
**Table 1: Osiris property explorer toxicity predictions**

Sr.No	Compound Code	Ar	Mutagenic	Tumorigenic	Irritant	Reproductive effect
1	C1	Phenyl	Green	Green	Green	Green
2	C2	4-Tolyl	Green	Green	Green	Green
3	C3	4-Ethylphenyl	Green	Green	Green	Green
4	C4	3,4-Dimethylphenyl	Green	Green	Green	Green
5	C5	3,4,5-Trimethylphenyl	Green	Red	Green	Green
6	C6	Pyridin-3-yl	Green	Green	Green	Green
7	C7	Furan-2-yl	Red	Green	Green	Green
8	C8	4-Chlorophenyl	Green	Green	Green	Green
9	C9	4-Hydroxyphenyl	Green	Green	Green	Green
10	C10	4-Hydroxy-3-methoxy-phenyl	Green	Green	Green	Green
11	C11	4-Hydroxy-3,5-dimethoxy-phenyl	Green	Green	Green	Green
12	C12	4-Methoxyphenyl	Green	Green	Red	Orange
13	C13	3,4-Dimethoxyphenyl	Green	Green	Green	Green
14	C14	3,4,5-Trimethoxyphenyl	Green	Green	Green	Green





Sr.No	Compound Code	Ar	Mutagenic	Tumorigenic	Irritant	Reproductive effect
15	C15	Phenyl	Green	Green	Red	Green
16	C16	4-Tolyl	Green	Green	Red	Green
17	C17	4-Ethylphenyl	Green	Green	Red	Green
18	C18	3,4-Dimethylphenyl	Green	Green	Red	Green
19	C19	3,4,5-Trimethylphenyl	Green	Red	Red	Green
20	C20	Pyridin-3-yl	Green	Green	Red	Green
21	C21	Furan-2-yl	Red	Green	Red	Green
22	C22	4-Chlorophenyl	Green	Green	Red	Green
23	C23	4-Hydroxyphenyl	Green	Green	Red	Green
24	C24	4-Hydroxy-3-methoxyphenyl	Green	Green	Red	Green
25	C25	4-Hydroxy-3,5-dimethoxyphenyl	Green	Green	Red	Green
26	C26	4-Methoxyphenyl	Green	Green	Red	Orange
27	C27	3,4-Dimethoxyphenyl	Green	Green	Red	Green
28	C28	3,4,5-Trimethoxyphenyl	Green	Green	Red	Green



S.No.	Compound Code	Ar	Mutagenic	Tumorigenic	Irritant	Reproductive effect
29	C29	Phenyl	Green	Green	Green	Green
30	C30	4-Tolyl	Green	Green	Green	Green
31	C31	4-Ethylphenyl	Green	Green	Green	Green
32	C32	3,4-Dimethylphenyl	Green	Green	Green	Green
33	C33	3,4,5-Trimethylphenyl	Red	Orange	Red	Green
34	C34	Pyridin-3-yl	Green	Green	Green	Green
35	C35	Furan-2-yl	Red	Green	Green	Green
36	C36	4-Chlorophenyl	Green	Green	Green	Green
37	C37	4-Hydroxyphenyl	Green	Green	Green	Green
38	C38	4-Hydroxy-3-methoxyphenyl	Green	Green	Green	Green
39	C39	4-Hydroxy-3,5-dimethoxyphenyl	Green	Green	Green	Green
40	C40	4-Methoxyphenyl	Green	Green	Red	Orange
41	C41	3,4-Dimethoxyphenyl	Green	Green	Green	Green
42	C42	3,4,5-Trimethoxyphenyl	Green	Green	Green	Green
43	Erlotinib	Reference	Green	Green	Green	Green
44	Afatinib	Reference	Green	Green	Green	Green
45	Naquotinib	Reference	Red	Red	Orange	Orange

Structural sites of the ligands responsible for the toxicities (predicted)

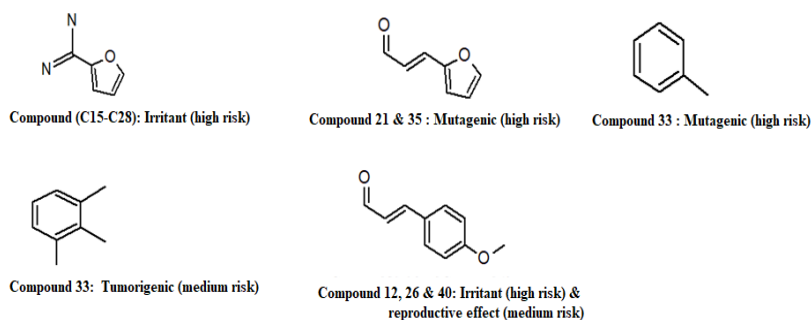


Fig. 1. Structural sites responsible for the toxicities (Osiris predictions)

The compound C5 is predicted as tumorigenic (high risk) by Osiris property explorer owing to the presence of ortho-dimethylphenyl site at the chalcone site. The compound C7 is predicted as mutagenic (high risk) by Osiris property explorer owing to the site 3-(furan-2-yl)prop-2-enoyl. As shown in Fig.1 the compound C12 is predicted as irritating (high risk) as well as it possesses deleterious reproductive effects (moderate risk) owing to the site 3-(4-methoxyphenyl)prop-2-enoyl. The compounds (C15-C28) possessing a 2-furyl substituent on the quinazolinone were predicted as irritants (high risk). The compound C21 besides irritant (high risk) is also predicted as mutagenic (high risk) owing to the site (2E)-3-(furan-2-yl)prop-2-enoyl. The compound 35 is also mutagenic (high risk) because of this site. The compound C33 besides being irritant (high risk) is also predicted as mutagenic (high risk) owing to the site 4-methylphenyl and is also tumorigenic (medium risk) because of its 3,4,5-trimethylphenyl site. The

compounds C12, C26, and C40 besides irritant (high risk) are also predicted to have a reproductive effect (medium risk) owing to the site (2E)-3-(4-methoxyphenyl)prop-2-enoyl.

#### Osiris property explorer drug score predictions

The drug score value combines all other predictions into one total. The drug score value takes into account several parameters viz. cLogP, logS, molweight, drug-likeness, and probable toxicity (mutagenicity, tumorigenicity, irritating effects, reproductive effects). The Osiris property explorer predicted a higher drug score for erlotinib (0.38) than afatinib (0.24), this prediction complies with the conclusion of the comparative clinical trial phase-3 studies between erlotinib and afatinib that concluded that the incidence of stomatitis and diarrhea, was more with afatinib when compared with erlotinib<sup>16</sup>. In the following table (Table 2), the ligands are arranged in descending order of their respective drug scores.

**Table 2: Osiris property explorer drug score prediction**

Compound Code	cLogP	Solubility	MW	TPSA	Drug likeness	Drug score
C6	4.6	-6.12	429	62.63	5.49	0.42
C9	5.25	-6.62	444	69.97	5.08	0.35
C10	5.18	-6.63	474	79.2	5.59	0.33
C34	5.2	-6.85	463	62.63	5.39	0.33
C11	5.11	-6.65	504	88.43	6.18	0.32
C1	5.6	-6.91	428	49.74	1.84	0.3
C13	5.46	-6.95	488	68.2	6.95	0.3
C20	3.79	-5.8	419	75.77	4.79	0.3
C2	5.94	-7.26	442	49.74	3.5	0.29
C14	5.39	-6.97	518	77.43	7.92	0.28
C37	5.86	-7.35	478	69.97	4.96	0.27
C3	6.36	-7.41	456	49.74	4.68	0.26
C8	6.21	-7.66	462	49.74	5.6	0.26
C38	5.79	-7.37	508	79.2	5.47	0.26
C4	6.29	-7.6	456	49.74	2.27	0.25
C23	4.44	-6.3	434	83.11	4.43	0.25
C29	6.21	-7.65	462	49.74	1.78	0.25
C39	5.72	-7.39	538	88.43	6.07	0.25
C24	4.37	-6.32	464	92.34	5	0.24
C30	6.55	-7.99	476	49.74	3.38	0.24
C41	6.07	-7.68	522	68.2	6.84	0.24
C7	4.79	-6.59	418	62.88	5.08	0.23
C25	4.3	-6.33	494	101.5	5.56	0.23
C42	6	-7.7	552	77.43	7.83	0.23
C27	4.65	-6.63	478	81.34	6.38	0.22
C31	6.97	-8.15	490	49.74	4.57	0.22
C36	6.81	-8.38	496	49.74	4.75	0.22
C15	4.79	-6.59	418	62.88	1.28	0.21
C28	4.58	-6.65	508	90.57	7.29	0.21
C32	6.89	-8.34	490	49.74	2.16	0.21
C16	5.13	-6.94	432	62.88	2.85	0.2
C17	5.55	-7.1	446	62.88	4.05	0.19

C22	5.39	-7.33	452	62.88	4.92	0.19
C35	5.39	-7.33	452	62.88	4.95	0.19
C26	4.72	-6.61	448	72.11	4.49	0.18
C18	5.48	-7.28	446	62.88	1.61	0.17
C21	3.98	-6.28	408	76.02	4.21	0.17
C5	6.63	-7.94	470	49.74	4.98	0.15
C12	5.53	-6.93	458	58.97	5.12	0.15
C40	6.14	-7.67	492	58.97	4.99	0.12
C19	5.82	-7.63	460	62.88	4.32	0.1
C33	7.24	-8.68	504	49.74	3.61	0.06
Erlotinib Reference	3.07	-3.53	393	74.73	-6.73	0.38
Afatinib Reference	3.64	-5.48	485	88.61	-4.11	0.24
Naquotinib Reference	2.54	-3.51	563	120.1	0.72	0.11

Osiris property explorer predicts that the compound C6 has the maximum drug score (0.42) among all the investigated compounds in the compound library and it is the only compound that has a drug score greater than the reference erlotinib (0.38; first generation EGFR inhibitor). In the library, eighteen compounds (C1- C4, C6, C8- C11, C13, C14, C20, C23, C29, C34, C37- C39) have greater drug score than the reference afatinib (0.24; second generation EGFR inhibitor). Except for C19 and C33, the other ligands have a greater drug score than naquotinib (0.11; third generation EGFR inhibitor).

#### Swiss ADME predictions for absorption, P-gp substrate, CYP enzymes inhibition

P-glycoprotein is a membrane transporter pump that is one of the main energy-dependent efflux mechanisms. P-glycoprotein effluxes many anticancer drugs out of the cells which can substantially reduce or demolish the activity and is one of the important reasons for drug resistance<sup>17</sup>. None of the ligands was found to be a P-glycoprotein substrate (Table 3), hence, the virtual investigations predict that none of the ligands would be effluxed by P-glycoprotein, from the tumor cells.

CYP superfamily enzymes are mainly expressed in the liver. Cytochrome P450 (CYP) enzymes play a primary role in metabolic phase-1 oxidative reactions that render the xenobiotics (drugs) hydrophilic by introducing polar handles and make them eligible for phase-2 metabolic reactions which subsequently make the drug pharmacodynamically neutral (i.e. termination of biological activity) and facilitates its renal clearance. CYP1A2 is involved in the metabolism of about 10% of clinically used drugs, except the ligand C21 none of the ligands is its inhibitors<sup>18</sup>. It implies that except

the ligand C21 (Table 3), no other ligand in the library slows down the metabolism of the drugs primarily metabolized by CYP1A2. In the present study, all the ligands (C1-C42) are found to be the inhibitors of the CYP2C19 enzyme (Table 3). Proguanil, rabeprazole, omeprazole, lansoprazole, pantoprazole, amitriptyline, clomipramine, amitriptyline, diazepam, S-mephenytoin, phenobarbitone, cyclophosphamide, clopidogrel, nelfinavir, and warfarin are among the drugs that primarily undergo oxidative metabolism by CYP2C19 enzyme<sup>19</sup>. Hence, all the ligands would slow down the metabolism of these drugs and slow down their renal clearance. CYP2C9 is one of the most important CYP superfamily enzymes, it has been estimated to contribute to the oxidative phase-1 metabolism of approximately 15% of all therapeutic agents that are subjected to biotransformation by CYP enzymes. The ligands C2-C5, C8, C19, C29-C33, C36, and C37 being non-inhibitors of CYP2C9 (Table 3) would not slow down the metabolism and renal excretion of those therapeutic agents (e.g. warfarin, ibuprofen, etc) primarily metabolized by CYP2C9 enzyme<sup>20</sup>. In the metabolism of a large number of clinically important drugs, the CYP2D6 enzyme act as a catalyst (~20% of commonly used therapeutic agents) including neuroleptics, antidepressants, antiarrhythmics, opioids, and lipophilic  $\beta$ -adrenoceptor blockers. In the present study, none of the ligands is found to be the inhibitor of CYP2D6 (Table 3) which implies that the ligands would not slow down the metabolism of the drugs primarily metabolized by CYP2D6<sup>21</sup>. CYP3A4 enzyme having unusually low substrate specificity is involved in the metabolism of about 60% of currently known therapeutics. The ligands C12-C14, C20, C21, C26-C28, C41 and C42 being inhibitors of CYP3A4 would slow down the metabolism of the varieties of the drugs which are metabolized by the CYP3A4 enzyme<sup>22</sup>.

**Table 3: Swiss ADME predictions for absorption, P-gp substrate, CYP enzymes inhibition**

Compound Code	Gastrointestinal absorption	Blood–brain-barrier permeant	Pgp substrate	Cyp1A2 inhibitor	Cyp2C19 inhibitor	Cyp2C9 inhibitor	Cyp2D6 inhibitor	Cyp3A4 inhibitor	Bioavailability Score	Alert for PAINS
C1	High	No	No	No	Yes	Yes	No	No	0.55	Zero
C2	High	No	No	No	Yes	No	No	No	0.55	Zero
C3	High	No	No	No	Yes	No	No	No	0.55	Zero
C4	High	No	No	No	Yes	No	No	No	0.55	Zero
C5	High	No	No	No	Yes	No	No	No	0.55	Zero
C6	High	No	No	No	Yes	Yes	No	No	0.55	Zero
C7	High	No	No	No	Yes	Yes	No	No	0.55	Zero
C8	High	No	No	No	Yes	No	No	No	0.55	Zero
C9	High	No	No	No	Yes	Yes	No	No	0.55	Zero
C10	High	No	No	No	Yes	Yes	No	No	0.55	Zero
C11	High	No	No	No	Yes	Yes	No	No	0.55	Zero
C12	High	No	No	No	Yes	Yes	No	Yes	0.55	Zero
C13	High	No	No	No	Yes	Yes	No	Yes	0.55	Zero
C14	High	No	No	No	Yes	Yes	No	Yes	0.55	Zero
C15	High	No	No	No	Yes	Yes	No	No	0.55	Zero
C16	High	No	No	No	Yes	Yes	No	No	0.55	Zero
C17	High	No	No	No	Yes	Yes	No	No	0.55	Zero
C18	High	No	No	No	Yes	Yes	No	No	0.55	Zero
C19	High	No	No	No	Yes	No	No	No	0.55	Zero
C20	High	No	No	No	Yes	Yes	No	Yes	0.55	Zero
C21	High	No	No	Yes	Yes	Yes	No	Yes	0.55	Zero
C22	High	No	No	No	Yes	Yes	No	No	0.55	Zero
C23	High	No	No	No	Yes	Yes	No	No	0.55	Zero
C24	High	No	No	No	Yes	Yes	No	No	0.55	Zero
C25	High	No	No	No	Yes	Yes	No	No	0.55	Zero
C26	High	No	No	No	Yes	Yes	No	Yes	0.55	Zero
C27	High	No	No	No	Yes	Yes	No	Yes	0.55	Zero
C28	High	No	No	No	Yes	Yes	No	Yes	0.55	Zero
C29	High	No	No	No	Yes	No	No	No	0.55	Zero
C30	High	No	No	No	Yes	No	No	No	0.55	Zero
C31	Low	No	No	No	Yes	No	No	No	0.55	Zero
C32	Low	No	No	No	Yes	No	No	No	0.55	Zero
C33	Low	No	No	No	Yes	No	No	No	0.17	Zero
C34	High	No	No	No	Yes	Yes	No	No	0.55	Zero
C35	High	No	No	No	Yes	Yes	No	No	0.55	Zero
C36	Low	No	No	No	Yes	No	No	No	0.55	Zero
C37	High	No	No	No	Yes	No	No	No	0.55	Zero
C38	High	No	No	No	Yes	Yes	No	No	0.55	Zero
C39	Low	No	No	No	Yes	Yes	No	No	0.55	Zero
C40	High	No	No	No	Yes	Yes	No	No	0.55	Zero
C41	High	No	No	No	Yes	Yes	No	Yes	0.55	Zero
C42	Low	No	No	No	Yes	Yes	No	Yes	0.55	Zero
Erlotinib	High	Yes	No	Yes	Yes	Yes	Yes	Yes	0.55	Zero
Reference Afatinib	High	No	Yes	No	Yes	Yes	Yes	Yes	0.55	Zero
Reference Naquotinib	High	No	Yes	No	No	No	No	Yes	0.17	One

### Docking, Docked pose and Binding with target protein

The respective .dlg files included the ligand's inhibition constant (KI) and free energy of binding (BE). The complex of the target protein and the ligand's best-fit pose was saved in the .pdb file. The Discovery studio software was used to see the binding posture of the ligand and its interactions with target protein.

In Molecular docking studies of 42 ligands, It was observed that all the ligands occupied the reported binding site of the target molecular protein5Y9T23 (Fig. 2). All the designed ligands exhibited good affinity for the molecular target protein 5Y9T as the free binding energies were observed in the range of -45.44 KJ/mol to -34.64 KJ/mol, the inhibition constants of the ligands were observed in the range of 11.04 nM to 853.47 nM (Table 4).

Table 4: Docking data

Compound	Ar	Docking Rank	Constant of Inhibition (IC) (in nM)	Binding Energy (in KJ/mol)	Hydrogen bonds	Hydrogen bonding amino acids (Bond distance in Å <sup>o</sup> )	Other interacting amino acids	No. of amino acids interacting
C1	Phenyl	22	127.35	-39.37	1	MET793(2.28)	LEU718,ALA743,VAL726,PHE723,ASP855,LEU792,LEU844,LYS728,PRO794	10
C2	4-Tolyl	13	49.16	-41.71	1	MET793(1.80)	ASP855,MET790,LEU718,PRO794,LEU792,ALA743,LEU844,VAL726,PHE723	10
C3	4-Ethylphenyl	11	40.19	-42.22	1	MET793(1.81)	MET790,PRO794,LEU792,ALA743,LEU718,LEU844,VAL726,PHE723,ASP855	10
C4	3,4-Dimethylphenyl	6	21.64	-43.76	1	MET793(1.76)	PRO794,LEU792,LYS728,LEU718,LEU844,ALA743,VAL726,PHE723,ASP855,MET790	11
C5	3,4,5-Trimethylphenyl	3	14.56	-44.73	1	MET793(1.68)	ALA743,LEU844,VAL726,MET790,ASP855,LYS728,LEU792,PRO794,LEU718	10
C6	Pyridin-3-yl	36	346.06	-36.86	1	MET793(2.44)	LEU718, VAL726,ASP855,MET790,LYS745,PRO794,LEU844	8
C7	Furan-2-yl	38	471.17	-36.11	1	MET793(2.38)	ALA743,LEU844,VAL726,ASP855,MET790,PRO794,LEU718	8
C8	4-Chlorophenyl	16	78.74	-40.54	1	MET793(2.33)	LEU844,VAL726,ASP855,LYS728,LEU792,PRO794	7
C9	4-Hydroxyphenyl	28	254.35	-37.66	1	MET793(2.07)	LEU844,ALA743,VAL726,PHE723,ASP855,PRO794,LEU792,LEU718	9
C10	4-Hydroxy-3-methoxyphenyl	15	69.25	-40.88	3	LYS716(2.10),LYS728(2.92),GLY796(2.64)	LEU718,GLY719,VAL726,MET790,ASP855,LYS745,LEU844	10
C11	4-Hydroxy-3,5-dimethoxyphenyl	14	60.47	-41.21	3	LYS716(2.24),LYS716(4.48),GLY796(2.58)	LEU718,GLY719,VAL726,ASP855,MET790,LEU844,VAL717,LYS728	10
C12	4-Methoxyphenyl	19	116.31	-39.58	1	MET793(2.17)	LEU844,ALA743,VAL726,PHE723,ASP855,LYS728,PRO794,LEU718	9
C13	3,4-Dimethoxyphenyl	18	89.47	-40.25	3	LYS716(4.91),LYS716(2.46),GLY796(2.79)	LEU718,GLY719,VAL726,MET790,ASP855,LEU844,LYS728	9
C14	3,4,5-Trimethoxyphenyl	17	84.59	-40.38	3	LYS716(2.01),LYS716(2.44),GLY796(2.88)	LEU718,GLY719,VAL726,PHE723,MET790,ASP855,LEU844,LYS728,VAL717	11
C15	Phenyl	32	286.74	-37.36	1	MET793(1.89)	PRO794,LEU718,ALA743,LEU792,GLN791,MET790,LEU844	8

C16	4-Tolyl	8	31.66	-42.8	2	MET793(1.84), LYS745(2.00)	PRO794, LEU792, LEU718, LEU844, ALA743, VAL726, SER720, PHE723, GLY721, ASP855, MET790	13
C17	4-Ethylphenyl	7	28.28	-43.1	2	MET793(1.80), LYS745(2.05)	PRO794, LEU792, LEU718, LEU844, ALA743, VAL726, ASP855, MET790	10
C18	3,4-Dimethylphenyl	4	14.5	-44.73	2	MET793(1.73), LYS745(1.97)	MET790, PRO794, LEU792, LYS728, ALA743, LEU718, LEU844, VAL726, ASP855	11
C19	3,4,5-Trimethylphenyl	1	11.04	-45.44	2	MET793(1.87), LYS745(2.02)	PRO794, LEU792, LYS728, LEU718, ALA743, LEU844, VAL726, PHE723, ASP855, MET790	12
C20	Pyridin-3-yl	33	293.59	-37.28	1	LYS745(1.83)	LEU844, LEU718, MET790, ALA743, LEU792, GLN791, ASP855, MET793	9
C21	Furan-2-yl	42	853.47	-34.64	1	MET793(1.97)	LYS728, PRO794, LEU792, LEU718, GLN791, ALA743, MET790, LEU844, VAL726	10
C22	4-Chlorophenyl	26	230.48	-37.87	2	MET793(1.99), LYS745(2.38)	SER720, VAL726, PHE723, GLY721, ASP855, MET790, LEU792, LYS716, LEU718, LYS728, LEU844, ALA743	14
C23	4-Hydroxyphenyl	41	589.14	-35.56	1	MET793(2.34)	ALA743, VAL726, ASP855, MET790, LEU844, PRO794, LEU718, LYS728	9
C24	4-Hydroxy-3-methoxyphenyl	40	561.85	-35.69	1	MET793(2.52)	LEU718, LEU844, VAL726, PHE723, ASP855, LEU792, PRO794, LYS728	9
C25	4-Hydroxy-3,5-dimethoxyphenyl	25	173.71	-38.58	3	LYS728(2.64), LYS716(1.95), GLY796(2.54)	LEU718, GLY719, PHE723, VAL726, ASP855, MET790, LEU844	10
C26	4-Methoxyphenyl	34	306.24	-37.2	1	MET793(2.11)	ALA743, LEU844, VAL726, PHE723, ASP855, MET790, LEU718, LYS728, PRO794	10
C27	3,4-Dimethoxyphenyl	30	265.5	-37.53	3	GLY796(2.70), LYS716(2.61), LYS716(2.97)	LEU718, LYS728, LEU792, ASP855, LEU844, VAL726, GLY719	9
C28	3,4,5-Trimethoxyphenyl	21	118.48	-39.54	2	LYS716(2.42), GLY796(2.72)	LEU844, GLY719, VAL726, LYS745, MET790, LEU718, LYS728, LEU792	10
C29	Phenyl	27	233.16	-37.87	1	MET793(3.00)	VAL726, GLY719, PHE723, ASP855, MET790, PRO794, LEU792, LYS728, LEU718	10
C30	4-Tolyl	10	39.61	-42.26	1	MET793(1.97)	LEU792, PRO794, LEU718, ALA743, LEU844, VAL726, SER720, PHE723, LYS745, ASP855, MET790, MET766, GLY721	14
C31	4-Ethylphenyl	9	35.56	-42.51	1	MET793(2.00)	LEU792, PRO794, LEU718, ALA743, LEU844, VAL726, PHE723, LYS745,	12



C32	3,4-Dimethylphenyl	5	15.89	-44.52	1	MET793(1.95)	ASP855,MET790,MET766 LEU718,PRO794,LEU792,LYS728, ALA743,LEU844,VAL726,PHE723, LYS745,ASP855,MET766,MET790 ALA743,LEU844,VAL726,MET790, ASP855,LYS728,LEU792,PRO794, LEU718	13
C33	3,4,5-Trimethylphenyl	2	13.04	-45.02	1	MET793(1.68)	LEU844,VAL726,GLY719,PHE723, ASP855,LYS745,MET790,PRO794 ASP837,CYS797,LEU718,LEU844, MET790,VAL726	10
C34	Pyridin-3-yl	35	322.13	-37.07	1	MET793(2.71)	LEU844,VAL726,GLY719,PHE723, ASP855,LYS745,MET790,PRO794	9
C35	Furan-2-yl	39	479.18	-36.07	1	ARG841(5.47)	ASP837,CYS797,LEU718,LEU844, MET790,VAL726	7
C36	4-Chlorophenyl	29	261.09	-37.57	1	MET793(2.68)	LEU844,VAL726,GLY719,PHE723, LYS745,ASP855,MET790,PRO794	9
C37	4-Hydroxyphenyl	24	128.44	-39.33	1	MET793(2.14)	LEU718,ALA743,LEU844,VAL726, PHE723,LYS745,MET766,MET790, PRO794	10
C38	4-Hydroxy-3-methoxyphenyl	37	356.01	-36.82	1	LYS716(2.77)	LEU844,GLY719,VAL726,ASP855, LYS745,MET790,LYS728	8
C39	4-Hydroxy-3,5-dimethoxyphenyl	20	116.49	-39.58	2	MET793(2.36),LYS716(2.50)	LEU718,LEU844,ALA743,GLY719, VAL726,PHE723,ASP855,MET790, LYS728	11
C40	4-Methoxyphenyl	31	273.28	-37.45	1	MET793(2.65)	GLY719,VAL726,PHE723,LYS745, ASP855,MET790,LEU844	8
C41	3,4-Dimethoxyphenyl	12	43.45	-42.01	1	MET793(1.86)	ALA743,LEU844,VAL726,LYS745, ASP855,MET766,MET790,LYS728, LEU792,PRO794,LEU718	12
C42	3,4,5-Trimethoxyphenyl	23	125.89	-39.37	3	LYS716(2.36),LYS716 (2.54),GLY796(2.71)	LEU718,GLY719,VAL726,ASP855, MET790,LYS745,LYS728	9
Reference Erlotinib			2.37 micro-molar	-32.13	3	LYS860 (1.88 & 2.48), GLU762 (1.86)	GLU758,ILE759,ALA755,LEU747, LYS745	7
Reference Afatinib			1.30 micro-molar	-33.60	2	MET793(1.87), CYS797(2.00)	ALA743,LEU792,LEU844,LEU718, ASP800,TYR801,PHE795	9
Reference Naquotinib			1.55 micro-molar	-33.18	3	ASP855(3.01),THR854 (2.26),CYS797(2.51)	LEU844,ALA743,VAL726,MET790, LEU718,ARG841,PHE723	10

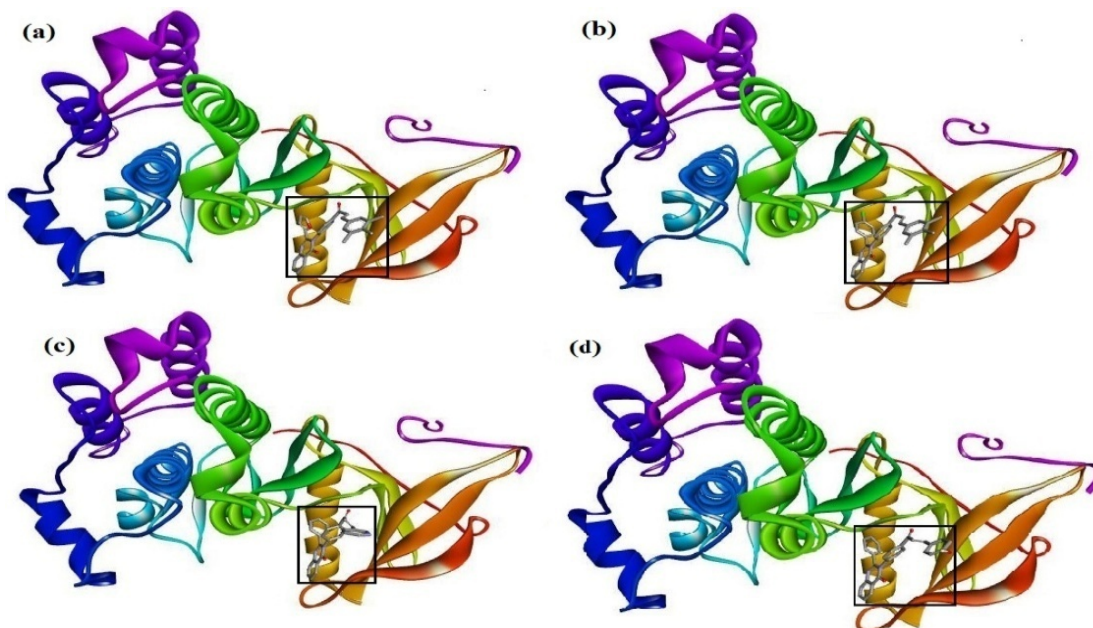


Fig. 2. Ligands binding with EGFR (5Y9T) (a) C19 (b) C33 (c) C6 (d) C9

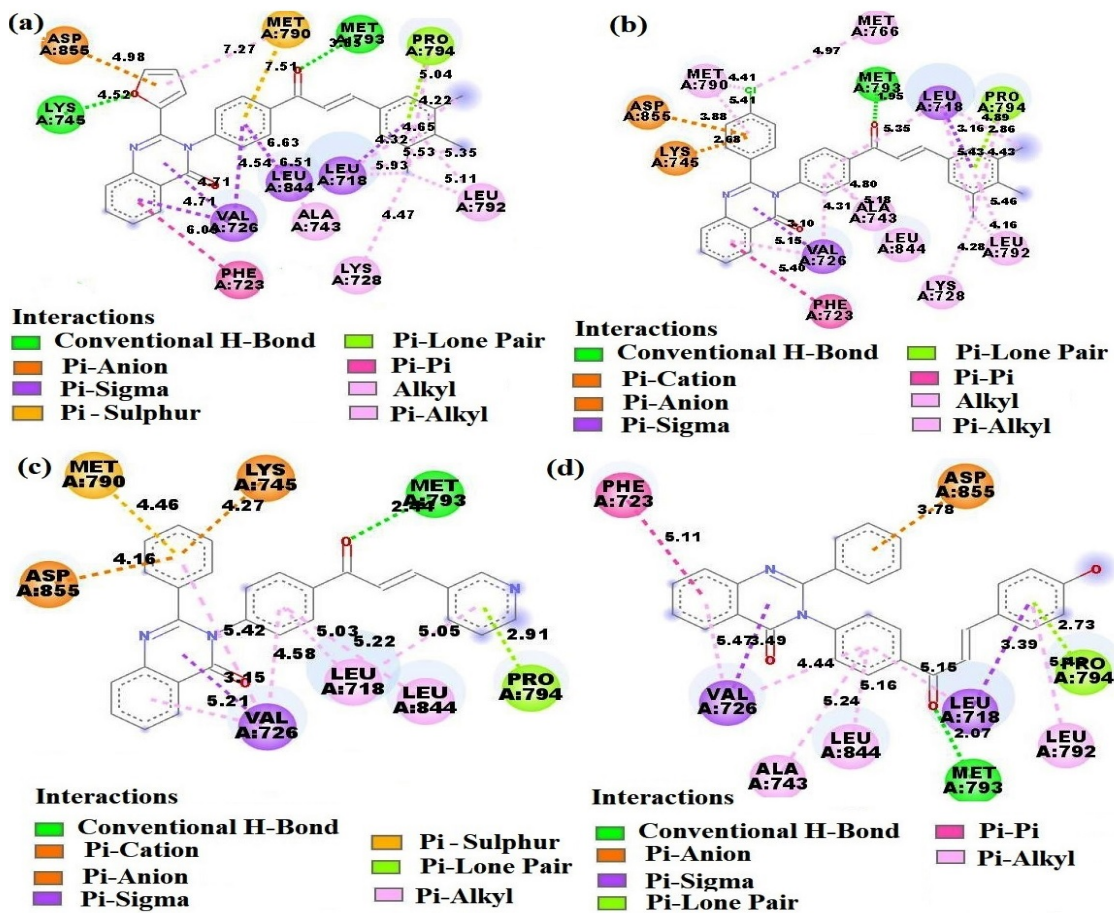


Fig. 3. Ligands interactions with EGFR (5Y9T) (a) C19 (b) C33 (c) C6 (d) C9

**C19 & C33 interactions (most potent ligands)**

*In silico* docking studies revealed that the compound C19 has the highest affinity (binding energy = -45.44 KJ/mol and inhibition constant = 11.04 nM) and the compound C33 was observed as 2<sup>nd</sup> most potent ligand (binding energy = -45.02 KJ/mol and inhibition constant = 13.04 nM) for the molecular target protein 5Y9T. The ligand-target interaction studies (Fig. 3), revealed that in both the highly potent ligands (compound C19 & compound C33) the carbonyl oxygen of the chalcone site acts as an H-bond acceptor with the MET793 amino acid while in compound C19 the oxygen of furan ring also acts as H-bond acceptor with LYS745 amino acid. The quinazolinone ring system makes Pi-Pi and Pi-sigma bindings with PHE723 and VAL726 respectively. The aromatic ring (furan in C19 and phenyl in C33) makes Pi-anion interaction with the carboxylate site of ASP855. The phenyl ring at N-3 of quinazolinone makes Pi-sigma and Pi-alkyl bonding with VAL726 and ALA743, respectively. The “3,4,5-trimethylphenyl” substituent on the beta-unsaturated carbon (w.r.t. carbonyl group of chalcone) makes Pi-lone pair binding with PRO794, Pi-sigma binding with LEU718 and alkyl/Pi-alkyl type of bindings with LYS728 and LEU792.

**C6 (highest drug score) & C9 (2nd highest drug score) interactions**

*In silico* docking studies revealed that the compound C6 has the binding energy = -45.44 KJ/mol and inhibition constant = 11.04 nM while the compound C9 has the binding energy = -45.02 KJ/mol and inhibition constant = 13.04 nM, for the molecular target protein 5Y9T. The ligand-target interaction studies (Fig. 3) revealed that in both the high drug score ligands (compound C6 & compound C9) the carbonyl oxygen of the chalcone site acts as an H-bond acceptor with the MET793 amino acid. The quinazolinone ring system makes Pi-sigma interaction with VAL726. 2-Phenyl substituent of quinazolinone makes Pi-anion interaction with the carboxylate site of ASP855. The phenyl ring at N-3 of quinazolinone makes a Pi-alkyl bond with LEU844. Aromatic substituents (pyridinyl in C6 and 4-hydroxyphenyl in C9) at the beta-unsaturated carbon (w.r.t. carbonyl group of chalcone) make Pi-lone pair interaction with PRO794.

The review of the literature showed that the requirement to treat NSCLC with T790M mutant EGFR remains a significant unmet need. Madhavi *et al.*, has reported certain “quinazoline

integrated chalcones derivatives” as strong cytotoxic agents against cancer cell lines (colorectal, breast, melanoma, and lung cancer), with an IC<sub>50</sub> range of 0.10 to 0.19 mM<sup>5</sup>. The molecular docking studies and invitro cytotoxic studies of quinazolinone-naphthyl chalcones and 2-methoxyquinazolinone chalcones have enlightened that quinazolinone-chalcone conjugates are potent anticancer agents and can be the promiscuous chemical entities to target T790M mutated EGFR<sup>10,11</sup>. Le *et al.*, discovered that the methyl substituted quinazolinone derivatives were potent inhibitors of wild-type EGFR, with IC<sub>50</sub> (mM) values ranging from 0.01-0.54<sup>24</sup>. Zhang *et al.*, observed that several analogs of 2-phenoxyethylquinazolinone were potent EGFR (wild-type) inhibitors, with IC50 values ranging from 0.047 to 2.71 (mM)<sup>25</sup>. The third-generation EGFR TKIs, such as naquotinib, osimertinib or lazertinib, raised hope for NSCLC patients with T790M mutation; however, these medications are associated with substantial side effects, and during treatment, patients develop EGFR resistance<sup>15,26</sup>. Thus, there is still a great unmet need for the treatment of NSCLC with the T790M mutant EGFR<sup>26</sup>. The present work involves the insilico exploration of low molecular weight chemical ligands for their drug score, toxicity, pharmacokinetic parameters, and their ability to inhibit mutated EGFR. As the explored ligands were not found to be the P-glycoprotein substrates (Table 3), none of the ligands would be effluxed by P-glycoprotein, from the tumor cells. The insilico exploration revealed that all the tested ligands are potent, have good target affinity, and have a good bioavailability Score. Moreover, the tested ligands have good synthesis feasibility<sup>10,11</sup>. The present research can be taken forward for the synthesis of ligands with high drug scores (e.g. C6 & C9) and good target affinity (e.g. C19 & C33) and their *in vitro/in vivo* evaluation for EGFR (T790M mutated) inhibition without wasting time, material, and money. Hence, the present insilico exploration gives momentum to the discovery of the drugs that can target mutated EGFRs, to defeat resistance hindrances.

**ACKNOWLEDGMENT**

This research did not receive any specific grant from funding agencies in the public, commercial, or not-for-profit sectors.

**Conflict of interest**

The author declare that we have no conflict of interest.

## REFERENCES

- Li, C.; Lei, S.; Ding, L.; Xu, Y.; Wu, X.; Wang, H.; Zhang, Z.; Gao, T.; Zhang, Y.; Li, L., *Chin Med J (Engl)*, **2023**, *136*(13), 1583-1590, doi: 10.1097/CM9.0000000000002529.
- Rebecca, L.S.; Kimberly, D.M.; Hannah, E.F.; Ahmedin, J., *CA Cancer J Clin*, **2022**, *72*, 7–33.
- Altamimi, A.S.; El-Azab, A.S.; Abdelhamid, S.G.; Alamri, M.A.; Bayoumi, A.H.; Alqahtani, S.M.; Alabbas, A.B.; Altharawi, A.I.; Alossaimi, M.A.; Mohamed, M.A., *Molecules*, **2021**, *26*(10), 2992, doi: 10.3390/molecules26102992.
- Ouyang, Y. Li. J.; Chen, X. Fu. X.; Sun, S.; Wu, Q., *Biomolecules*, **2021**, *11*(6), 894, doi: 10.3390/biom11060894.
- Madhavi, S.; Sreenivasulu, R.; Yazala, J.P.; Raju, R.R., *Saudi Pharm J*, **2017**, *25*, 275-279.
- Abbas, S.H.; Abd El-Hafeez, A.A.; Shoman, M.E.; Montano, M. M.; Hassan, H.A., *Bioorg Chem*, **2019**, *82*, 360-377.
- Zhou, W.; Zhang, W.; Peng, Y.; Jiang, Z.H.; Zhang, L.; Du, Z., *Molecules*, **2020**, *25*, 3180-3197.
- Kasetti, A.B.; Singhvi, I.; Nagasuri, R.; Bhandare, R.R.; Shaik, A.B., *Molecules*, **2021**, *26*, 2847-2862.
- Alam, M. J.; Alam, O.; Perwez, A.; Rizvi, M.A.; Naim, M.J.; Naidu, V.G.M.; Imran, M.; Ghoneim, M.M.; Alshehri, S.; Shakeel, F., *Pharmaceuticals (Basel)*, **2022**, *15*, 280-299.
- Arora, P.K.; Kumar, S.; Bansal, S.K.; Sharma, P. C., *Orient J Chem*, **2023**, *39*(2), 231-245.
- Arora, P.K.; Kumar, S.; Bansal, S.K.; Sharma, P. C., *Rasayan J. Chem*, **2023**, *16*(3), 1104-1115.
- Bao, S.M.; Hu, Q.H.; Yang, W.T.; Wang, Y.; Tong, Y.P.; Bao, W.D., *Anticancer Agents Med Chem*, **2019**, *19*, 984-991.
- Xie, Y.H.; Chen, Y.X.; Fang, J.Y., *Signal Transduct Target Ther*, **2020**, *5*, 22-34.
- Peng, W.; Yao, C.; Pan, Q.; Zhang, Z.; Ye, J.; Shen, B.; Zhou, G.; Fang, Y., *Front Oncol*, **2023**, *13*, 1120278, doi:10.3389/fonc.2023.1120278.
- Boch, T.; Köhler, J.; Janning, M.; Loges, S., *Cancer Biol Med*, **2022**, *19*(11), 1543–64, doi:10.20892/j.issn.2095-3941.2022.0540.
- Soria, J.C.; Felip, E.; Cobo, M.; Lu, S.; Syrigos, K.; Lee, K.H.; Göker, E.; Georgoulas, V.; Li, W.; Isla, D.; Guclu, S.Z.; Morabito, A.; Min, Y.J.; Ardizzoni, A.; Gadgeel, S.M.; Wang, B.; Chand, V.K.; Goss, G.D., *Lancet Oncol*, **2015**, *16*, 897-907.
- Heming, C. P.; Muriithi, W.; Wanjiku, M. L.; Niemeyer, F. P.; Moura-Neto, V.; Aran, V., *Heliyon*, **2022**, *8*(10), e11171. doi: 10.1016/j.heliyon.2022.e11171.
- Esteves, F.; Almeida, C.M.M.; Silva, S.; Saldanha, I.; Urban, P.; Rueff, J.; Pompon, D.; Truan, G.; Kranendonk, M., *Biomolecules*, **2023**, *13*(7), 1083, doi:10.3390/biom13071083.
- Botton, M.R.; Whirl-Carrillo, M.; Del, T. A.L.; Sangkuhl, K.; Cavallari, L.H.; Agúndez, J.A.G.; Duconge, J.; Lee, M.T.M.; Woodahl, E.L.; Claudio-Campos, K.; Daly, A.K.; Klein, T.E.; Pratt, V.M.; Scott, S.A.; Gaedigk, A., *Clin Pharmacol Ther*, **2021**, *109*(2), 352-366, doi: 10.1002/cpt.1973.
- Sangkuhl, K.; Claudio-Campos, K.; Cavallari, L.H.; Agúndez, J.A.G.; Whirl-Carrillo, M.; Duconge, J.; Del Tredici, A.L.; Wadelius, M.; Rodrigues, B. M.; Woodahl, E.L.; Scott, S.A.; Klein, T.E.; Pratt, V.M.; Daly, A.K.; Gaedigk, A., *Clin Pharmacol Ther*, **2021**, *110*(3), 662-676, doi: 10.1002/cpt.2333.
- Taylor, C.; Crosby, I.; Yip, V.; Maguire, P.; Pirmohamed, M.; Turner, R.M., *Genes (Basel)*, **2020**, *11*(11), 1295, doi:10.3390/genes11111295.
- Klyushova, L.S.; Perepechaeva, M.L.; Grishanova, A.Y., *Biomedicines*, **2022**, *10*(11), 2686, doi: 10.3390/biomedicines10112686.
- Hirano, T.; Yasuda, H.; Hamamoto, J.; Nukaga, S.; Masuzawa, K.; Kawada, I.; Naoki, K.; Niimi, T.; Mimasu, S.; Sakagami, H.; Soejima, K.; Betsuyaku, T., *Mol Cancer Ther*, **2018**, *17*, 740-750.
- Le, Y.; Gan, Y.; Fu, Y.; Liu, J.; Li, W.; Zou, X.; Zhou, Z.; Wang, Z.; Ouyang, G.; Yan, L., *J Enzyme Inhib Med Chem*, **2020**, *35*, 555-564, doi:10.1080/14756366.2020.1715389.
- Zhang, Y.; Wang, Q.; Li, L.; Le, Y.; Liu, L.; Yang, J.; Li, Y.; Bao, G.; Yan, L., *J Enzyme Inhib Med Chem*, **2021**, *36*, 1205-1216.
- Agema, B.C.; Veerman, G.D.M.; Steendam, C.M.J.; Lanser, D.A.C.; Preijers, T.; Van der Leest, C.; Koch, B.C.P.; Dingemans, A.C.; Mathijssen, R.H.J.; Koolen, S.L.W., *Ther Adv Med Oncol*, **2022**, *14*, 1-10.